ACS Catalysis

Review

pubs.acs.org/acscatalysis

H_2S-Selective Catalytic Oxidation: Catalysts and Processes

Xin Zhang,[†] Yuyin Tang,[†] Siqiu Qu,[‡] Jianwen Da,[§] and Zhengping Hao*[,†]

[†]Department of Environmental Nano-materials, Research Center for Eco-Environmental Sciences, Chinese Academy of Sciences, Beijing 100085, People's Republic of China

[‡]Center of Research & Development, Shandong Sunway Petrochemical Engineering Share Co., Ltd., Beijing 100015, People's Republic of China

[§]Sinopec Qilu Co., Zibo 255400, People's Republic of China

ABSTRACT: The most widely used catalysts and processes for H_2S-selective catalytic oxidation are overviewed in this review. Two kinds of catalysts have been investigated intensively: carbon-based catalysts (active carbon catalyst, carbon nanotube catalyst, and carbon nanofiber catalyst), metal oxide-based catalysts (metal oxide catalyst, oxide-supported catalyst, and clay-supported catalyst). Among them, carbon-based catalysts are utilized mainly in discontinuous processes at relatively low temperatures, whereas metal oxide catalysts are the most widely used in practice. However, the reaction temperature is relatively high. Fortunately, a MgAlVO catalyst derived from LDH materials and intercalated clay-supported catalysts exhibit excellent catalytic activities at relatively lower temperatures. According to various studies, the catalytic behaviors mainly obey the Mars−van Krevelen mechanism; however, the catalyst deactivation mechanism differs, depending on the catalyst. In practice, the mobil direct oxidation process (MODOP), super-Claus and Euro-Claus processes were developed for H_2S-selective catalytic oxidation. Nevertheless, MODOP has to proceed under water-free conditions. The super-Claus process can operate in up to 30% water content. The Euro-Claus process is a modified version of the super-Claus process, which was developed to eliminate recovery losses of escaped SO_2.

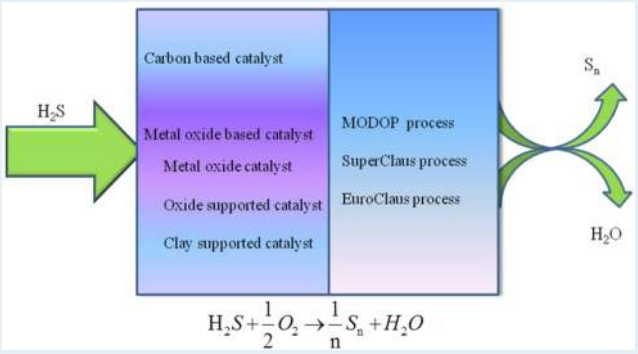

KEYWORDS: *H_2S-selective catalytic oxidation, catalyst, catalytic mechanism, catalyst deactivation, catalytic process*

1. INTRODUCTION

Hydrogen sulfide (H_2S) is one of the most toxic and malodorous gases emitted, largely from chemical industries, such as natural gas processing and utilization, hydrodesulfurization of crude oil, and coal chemistry. H_2S is harmful to animals and human beings.[1−3] People die when the H_2S > 700 ppm.[4] Moreover, H_2S, in both a gaseous form and in solution, is extremely corrosive to piping and production facilities.[5]

Because of the ever increasing efficiency standards required for environmental protection, sulfur-containing gas must be treated prior to its emission into the atmosphere. The most widely used technology now is the Claus process, which recovers elemental sulfur from sulfur-containing gas. The Claus process was first presented by Claus in a patent in 1883[6] and then was improved and researched significantly.[7,8] Most of the Claus process uses H_2S, CO_2, and H_2O as the main components and N_2, NH_3, and hydrocarbons as secondary components.[9] Figure 1[10] shows a schematic of the Claus process, which involves two reaction stages.

In the first stage, one-third of the initial H_2S is transformed to SO_2 in a combustion chamber at 1000−1200 °C

$$H_2S + \frac{3}{2}O_2 \rightarrow SO_2 + H_2O \quad (1)$$

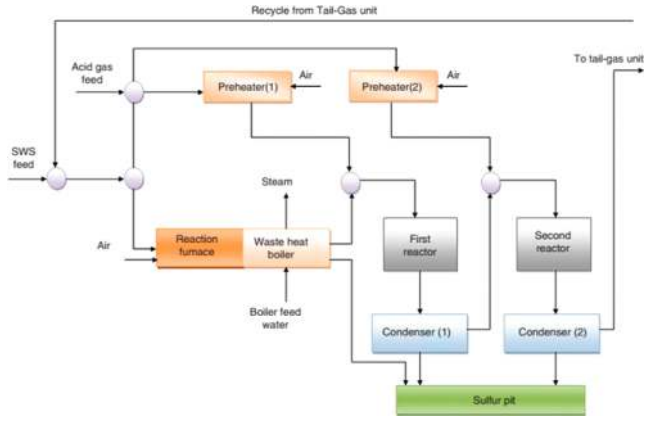

Figure 1. Flow diagram of two-stage Claus process.[10] Figure reproduced from ref 10 with permission from John Wiley and Sons, Copyright 2002.

The subsequent reaction converts part of the acid gas to sulfur

Received: September 27, 2014
Revised: December 3, 2014
Published: December 26, 2014

DOI: 10.1021/cs501476p
ACS Catal. 2015, 5, 1053−1067

Table 1. Comparison of Three Kinds of Claus Tail Gas Treatment Technologies

process	low-temperature Claus method	reduction−absorption method	H_2S-selective catalytic oxidation method
mechanism	the tail gas (H_2S and SO_2) further proceeds in the Claus reaction in low temperature (usually 130 °C, below the sulfur dew point) over a special catalyst	the sulfur compounds were hydrogenated to H_2S and then selective absorption using MEDA solution; after steam stripping, H_2S was returned to proceed in the Claus reaction	H_2S directly react with O_2 over a suitable catalyst to product elemental sulfur
sulfur yield	98.5−99.5%	≥99.8%	98.5−99.5%
sulfur content	>1500 ppm	<300 ppm	>1500 ppm
cost	low	high	low

$$SO_2 + 2H_2S \rightarrow 2H_2O + \frac{3}{n}S_n \quad (2)$$

In the second stage, SO_2 and H_2S are further transformed catalytically into elemental sulfur in a series of reactors, followed by reaction 2.

Because of thermodynamic limits, the sulfur yield during the first stage is 60−70%. Using a suitable catalyst in the second stage leads to a higher sulfur yield. H_2S conversion can reach 98% if three reactors are used. The second stage is much less exothermic than that of reaction 1, which has led to large-scale industrial development of the Claus process.

Nevertheless, reasonably efficient removal of H_2S from the gas flow is difficult because of thermodynamic limitations, because 3−5% of the H_2S is left in the tail gas. Various additional purification processes based on adsorption, absorption, wet oxidation, and dry catalytic technology have been developed to treat the tail gas. Among these processes, three kinds of technology, including low-temperature Claus reaction technology, reduction−absorption technology, and H_2S selective catalytic technology, have been investigated intensively and applied. In the low-temperature Claus reaction technology, H_2S and SO_2 in the tail gas further proceed in the Claus reaction at a low temperature (usually 130 °C, below the sulfur dew point) in a liquid system over a special catalyst. The Claus reaction is preferred to generate more elemental sulfur because of the low reaction temperature. However, the catalysts have to be replaced periodically because of the deposition of produced liquid elemental sulfur on the catalysts surface. In the case of reduction−absorption technology, sulfur compounds are first hydrogenated to H_2S, followed by selective absorption using MDEA (methyldiethanolamine) solution. The desorbed H_2S is recycled to the Claus unit for sulfur recovery using the shell Claus off-gas treating process. H_2S selective catalytic oxidation technology has been of great research interest in recent decades because it involves catalytically oxidizing H_2S to elemental sulfur directly and is thermodynamically complete. The irreversible reaction equations are as follows (eq 3 is the main reaction and eqs 4 and 5 are side reactions):

$$H_2S + \frac{1}{2}O_2 \rightarrow \frac{1}{n}S_n + H_2O \quad (3)$$

$$\frac{1}{n}S_n + O_2 \rightarrow SO_2 \quad (4)$$

$$H_2S + \frac{3}{2}O_2 \rightarrow SO_2 + H_2O \quad (5)$$

More detailed information on the three treatment technologies is shown in Table 1. Among them, the H_2S-selective catalytic oxidation technology is a highly promising approach as a result of its thermodynamic completeness; however, the key feature is development of a new catalyst that prevents the reverse Claus reaction and deep oxidation of elemental sulfur to SO_2. Catalytic H_2S oxidation can be performed above or below the sulfur dew point (180 °C), that is, the process is continuous when the temperature is >180 °C. However, it is a discontinuous process when the temperature is <180 °C. The elemental sulfur formed during the discontinuous process is condensed within the catalyst micropores, and periodic regeneration is required to remove this deposited sulfur. Therefore, the catalyst plays a dual role: as a catalyst for direct oxidation of H_2S by air as well as an adsorbent for removing sulfur via chemisorption and maintaining it within the pore structure for easy sorbent disposal. Carbon materials are the most suitable catalysts for this process because of their high specific surface area and rich surface chemistry. A large number of other materials, such as metal oxides and clay, have been investigated intensively for H_2S-selective oxidation as a continuous process.

2. CATALYSTS FOR H_2S-SELECTIVE OXIDATION

2.1. Carbon-Based Catalysts. *2.1.1. Active-Carbon-Based Catalysts.* The possibility of using carbon as a catalyst has been proposed for some time.[11] In the 1920s, IG Farbenindustrie suggested purifying sulfur-containing gases over an activated carbon catalyst at temperatures <150 °C. As mentioned above, this is a discontinuous process involving a relatively low H_2S concentration (1000 ppm), and the O_2/H_2S concentration is much higher than the stoichiometric ratio, even with a 30-fold excess of oxygen. However, the catalyst must be regenerated repeatedly.

Microporous activated carbon has been well studied as an adsorbent/catalyst at temperatures of 20−70 °C.[12−15] In particular, the preferred temperature is suggested to be <150 °C, considering the catalytic activity and sulfur selectivity. It was revealed that catalytic oxidation of H_2S requires large-pore carbon with a high total pore volume with respect to adsorptive desulfurization, which requires small pores. Furthermore, the micropores must be interconnected with mesopores (and macropores) for the sulfur adsorbed in the micropores to be accessible for SO_2 oxidation (and subsequent formation of H_2SO_4). Further research showed that the elemental sulfur formed was deposited preferentially in pores with diameters <12 Å as a result of the capillary effect. After the small capillaries were filled, the capillaries with larger diameters started to fill. Moreover,[16−18] the closer the pore width is to the size of the adsorbate molecule, the stronger the adsorption force. Therefore, a good carbon material should possess a desired microstructure, such as high volumes of both micropores and small mesopores, in combination with a relatively narrow pore size distribution for sulfur selectivity; however, the influences of pore size and pore volume on H_2S-selective catalytic oxidation are still not completely clear.

Notably, water vapor plays an important role in the discontinuous H_2S-selective catalytic oxidation process,[14]

DOI: 10.1021/cs501476p
ACS Catal. 2015, 5, 1053−1067

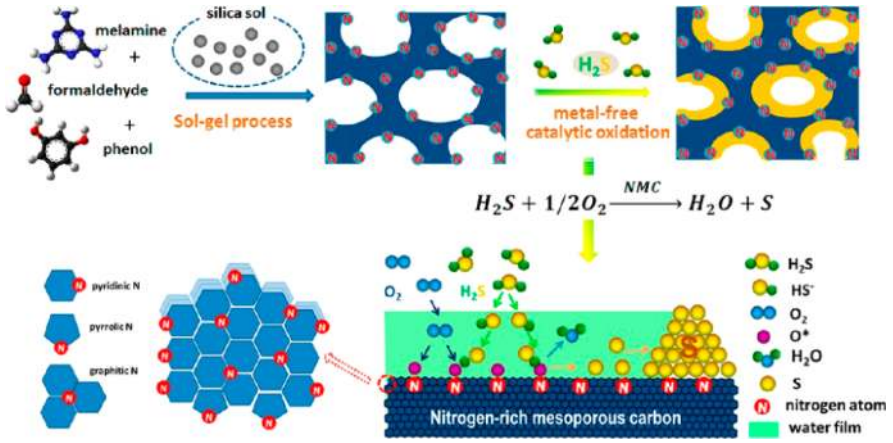

Figure 2. Schematic fabrication of NMC for the direct oxidation of H_2S and the possible reaction process.[44] Figure reproduced from ref 44 with permission from the American Chemical Society, Copyright 2013.

because water enhances the reaction rate efficiently. In particular, water improves the reaction rate at a relative humidity (RH, %) value of ~20%. Lower or higher water content does not produce the same enhanced reaction rate; however, catalytic performance decreases rapidly at RH values of 0−20. A less marked decrease in catalytic performance is displayed at RH > 75%. It has been further suggested that both the water present in feed gas and initially in the catalyst influence catalytic performance. Complete exhaustion of carbon cannot occur until the feed gas has a RH value of at least 50%. The important role of water in the reaction process can be explained by the remarkably different catalytic mechanism:[19] the O_2 are adsorbed on the carbon surface and cracked into reactive radicals through the water film. Meanwhile, H_2S dissolves in the water film to form HS^-, which further reacts with reactive oxygen radicals to produce elemental sulfur.

In contrast, the surface chemistry (such as basicity/acidity) of activated carbon can also govern catalytic activity greatly,[20] and many approaches have been developed to modify carbon materials. Among them, the most common ways to modify the carbon surface are impregnation with metal salts,[21] impregnation with alkaline chemicals[22−24] (sodium or potassium hydroxide, sodium or potassium carbonate, or iodide and potassium permanganate), introducing heteroatoms (such as oxygen, hydrogen, nitrogen, and phosphorus) and controlled oxidation and thermal treatment of carbon materials.[25−27] Three types of oxygen-containing groups (C═O type oxygen, C−O type oxygen, and charged oxygen O^-) can be incorporated effectively into the carbon surface by HNO_3 treatment.[28−30] Among these groups, charged oxygen species are related to relatively high catalytic activity. Modified carbon can oxidize 1.7−1.9 g H_2S/g catalyst at 180 °C during a one-operation cycle. This capacity exceeds the results reported using carbon catalysts in the literature.[15,31−33] However, deactivation of the catalyst was due mainly to deposition of elemental sulfur and a decrease in charged oxygen content with respect to an increase in C═O type oxygen. In contrast, treating the carbon with urea followed by calcining in nitrogen at different temperatures introduces various nitrogen compounds into the carbon matrix, which causes the surface pH to rise (pH = 6.7).[20] Moreover, the distinctive feature of carbon modified by urea is the presence of highly dispersed nitrogen groups in small pores. The HS^- ions contact the carbon matrix directly, which promotes the immediate creation of active sulfur radicals and superoxide ions[34] as a result of enhanced electron-transfer reactions on nitrogen-containing carbons. Interestingly, the dominant product is a water-soluble sulfur species. However, a remarkably different phenomenon is observed with Na_2CO_3- and NaOH-modified carbon. The surface of Na_2CO_3-modified carbon has a relatively higher pH compared with that of urea-modified carbon. The main product is elemental sulfur with little sulfuric acid. Moreover, Na_2CO_3 and NaOH are in abundance mainly in the liquid phase in pores. Na_2CO_3-modified carbon[35,36] has a highly beneficial effect on H_2S-selective oxidation. The sulfur capacity of the modified carbon is as high as 420 mg H_2S/g with a RH value of 80% at 30 °C. Modifying with Na_2CO_3 results in a high concentration of hydrosulfide ion (HS^-) and enhances H_2S oxidation. This high catalytic activity allows the pores to be utilized fully, which is the reason for the high sulfur capacity of modified carbon. Furthermore, the relatively higher pH prevents deactivation of the catalyst by the decrease of pH.

The breakthrough capacity of activated carbon becomes low as temperature increases, because a higher temperature results in poor efficiency and selectivity to produce COS and SO_2. Therefore, metal oxide is used to modify the carbon material using an impregnation method to promote sulfur capacity and catalytic performance at a relatively higher temperature.[21] Notably, catalytic activity decreases in the following order at 180 °C in the absence of water: Mn/AC > Cu/AC > Fe/AC > Ce/AC > Co/AC > V/AC. The capacity for Mn/AC is up to 142 mg H_2S/g, whereas that of V/AC is only 6.15 mg H_2S/g,. Elemental sulfur is the dominant product of H_2S catalytic oxidation on these catalysts. Moreover, the micropores of activated carbon and metal oxides on the sorbent surface are active centers for H_2S oxidation. The catalyst deactivation is mainly due to blockage of the micropores of activated carbon by elemental sulfur.

When CO is present in the raw gas, it will interact with sulfur to form the byproduct COS,[18,37,38] which is also formed via the interaction of H_2S with CO_2. According to a report by George,[39] depositing 3.9 wt % NaOH on active carbon increases COS adsorption efficiently from 0.011 to 0.018 mmol/g and also increases the initial rate of COS hydrolysis by 25-fold at 230 °C. Furthermore, impregnation with NaOH benefits H_2S conversion because NaOH facilitates the dissociation of H_2S into hydrosulfide ions (HS^-), which is followed by oxidization to elemental sulfur and to SO_2 and sulfuric acid (H_2SO_4). In contrast, OH^- groups can be introduced onto the carbon surface by NaOH impregnation, which increases retention of both SO_2[32,40−43] and

DOI: 10.1021/cs501476p
ACS Catal. 2015, 5, 1053−1067

COS, because COS can be adsorbed onto the surface via ion−dipole interactions between COS and OH^-.

Furthermore, the reaction temperature, O_2/H_2S ratio, space velocity (SV), and length-to-diameter ratio of the catalyst bed[18] also can strongly determine the activity and selectivity of active carbon. However, intrinsic problems associated with activated carbon include small micropores and low pore volume, which limit sulfur capacity to 0.2−0.6 g H_2S/g for caustic impregnated activated carbon and to 1.7−1.9 g H_2S/g for oxygen groups containing activated carbon. The relatively low sulfur saturation capacity necessitates frequent replacement of carbon catalysts associated with the low self-ignition temperature of alkali-modified carbon, and the difficulty with regeneration limits further applicability.

Nitrogen-rich mesoporous carbon with both a high surface density of catalytic sites and high pore volume for sulfur storage was developed using a colloidal silica-assisted sol−gel process.[44] The N content and N form play important roles in the process; when N content is 8%, sulfur capacity can be as high as 2.77g H_2S/g at 30 °C with a RH value of 80%. This can be attributed to pyridinic N. Because N atoms located at the edges of graphene sheets have strong electron-accepting ability, they are favorable for adsorbing oxygen atoms, which facilitates the oxidation reaction. Moreover, the basicity of the water film increases significantly as a result of the presence of nitrogen groups in the form of Lewis basic sites, which facilitate dissociation of H_2S into HS^- ions (pK =6.89). The nitrogen content in nitrogen-rich mesoporous carbon is highly critical because it dictates the basic properties that determine HS^- ion concentration. The preparation of nitrogen-rich mesoporous carbon and the proposed catalytic mechanism are briefly shown in Figure 2.

2.1.2. Carbon Nanotube-Based Catalysts. Carbon nanostructures, nanotubes, and nanofibers have received increasing interest since the first discovery of nanotubes in 1991.[31,45] Particularly for nanotubes, the completely absent microporosity in conjunction with the various structures (internal or external diameter and number of graphene layers) and rich surface chemistry (heterogeneous atoms or surface defects) makes them a promising material compared with microporous activated carbon, in which the large number of micropores increases diffusion greatly. Notably, the tubular morphology of carbon nanotubes can cause peculiar reactivity among gaseous or liquid reactants when passing through the tubules, for example, a confinement effect,[46] and the chemical inertness of carbon nanotubes avoids sulfation efficiently.

Metal oxide, alkaline chemicals, and heteroatoms are also often used to modify carbon nanotubes (CNTs). According to the literature,[31,46,47] Ni_2S-modified CNTs possess a high sulfur capacity of up to 1.80 g H_2S/g catalyst at 60 °C in trickle-bed mode. The Ni_2S active sites are all located inside the tube because of the confinement effect, and condensed water acts as a conveyor belt to transfer elemental sulfur from the inner to the external graphene sheet of multiwalled nanotubes, where they are free of the active phase. It, associated with the high activity of Ni_2S active sites, is responsible for high desulfurization activity without any deactivation after a 70-h reaction. The large free volumes of multiwalled carbon nanotubes for storage produce elemental sulfur and contribute to the high sulfur capacity. However, the hydrophobic properties of the Ni_2S/CNTs require condensed water to maintain high activity, which increases the difficulties in designing and manufacturing a reactor.

In contrast, Na_2CO_3-modified, single-walled CNTs[48] also obtain 1.86 g H_2S/g catalyst at a relatively lower temperature (30 °C), which is 3.9-fold higher than that of the referenced commercial desulfurizing commercially active carbon (0.48 g H_2S/g catalyst). Similar to a NiS_2/CNTs catalyst, sulfur capacity originates from the large stored volume, which is provided by the unique outside void of the CNT aggregates. Moreover, incorporation of the Na_2CO_3 enhances the hydrophilicity and alkalinity of the CNTs rather than acting as a catalyst. Alkalinity promotes sorption and dissociation of H_2S into HS^- ions in the water film. The decrease in pH caused by the sulfate formed and the blockage by elemental sulfur result in deactivation of the catalyst.

Because macroscopic N-CNTs[49] were developed and first used for H_2S-selective oxidation at high temperature (>180 °C) and high weighted hourly space velocity (WHSV) (0.2−1.2 h^{-1}, usually 0.09 h^{-1}), they were aimed at tackling the pressure drop problem. H_2S conversion increases with increased nitrogen concentration incorporated into the CNT matrix, which is attributed to the higher density of active sites for oxygen adsorbed on the N-CNTs. However, a reverse trend was observed for sulfur selectivity. H_2S conversion is 99.8% with respect to rather poor sulfur selectivity (10%) for a 2.6 wt %-containing catalyst at 250 °C. A 91% H_2S conversion and 75% sulfur selectivity can be attained when the temperature drops to 190 °C. Moreover, catalytic performance improves significantly when N-CNT is loaded onto SiC foam as a result of the higher spatial distribution of the N-CNTs. The catalyst exhibits excellent stability: both H_2S conversion and sulfur selectivity are 90% after a 120 h reaction at 190 °C with high WHSV. The proposed catalytic mechanism is displayed in Figure 3.

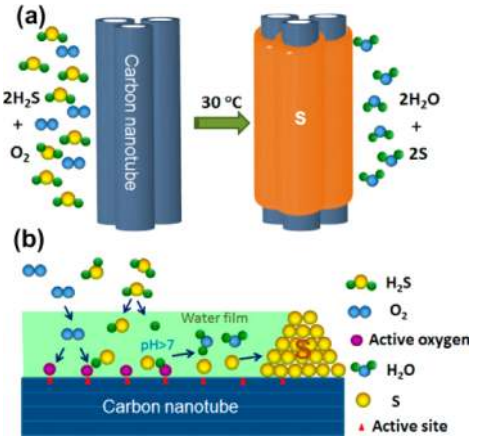

Figure 3. Schematic representation of H_2S oxidation over the alkaline CNTs: (a) the total reaction process and (b) the detailed reaction step.[48] Figure reproduced from ref 48 with permission from Elsevier, Copyright 2011.

2.1.2. Carbon Nanofiber-Based Catalysts. Similar to nanotubes, the main advantages of carbon nanofiber catalysts are their high thermal conductivity, excellent chemical inertia, and the absence of ink-bottle pores.[50] Moreover, the nonstructural pores of these materials, formed of microvoids between the nanofibers, have the additional advantage of higher sulfur uptake capacity.[51]

Applying the NFC for H_2S-selective catalytic oxidation at high temperature (>180 °C) has been investigated intensively compared with that of CNT catalysts. NFC is a promising candidate catalyst with respect to stoichiometric content, even at 30-fold excess oxygen.[52,53] However, catalytic performance is remarkably different with respect to various initial metal catalysts.

DOI: 10.1021/cs501476p
ACS Catal. 2015, 5, 1053−1067

In the absence of water, the NFC samples most selective to sulfur are those synthesized over Fe−Ni based catalysts[54] (with a nanofiber structure of multiwalled carbon nanotubes). Sulfur selectivity is consistent at 90%, whereas the H_2S conversion drops to 65% after a 25 h reaction. The most active samples are produced over Ni−Cu catalysts with a 95% H_2S conversion and 70% sulfur selectivity after a 25 h of reaction. In contrast, Ni-based NFC has a rather poor catalytic performance as a result of deposition of the S_8 clusters produced. Fortunately, Ni-based NFC has been modified with HNO_3 and NH_3[55] to improve catalytic performance. Acid treatment leads to increased stability. More importantly, a significant increase in sulfur selectivity is observed, which is mainly due to removing most of the active nickel from the carbon sample. However, NH_3 treatment decreases sulfur selectivity because this treatment makes active sites favorable for the deep oxidation of H_2S to the SO_2 formed. Notably, the catalytic performance is enhanced significantly in the presence of 40% water, particularly for the unmodified Ni-based NFC (70% H_2S conversion and 89% sulfur selectivity). Water adsorbs onto these active sites, preventing adsorption of sulfur.

Many studies have focused on low-temperature H_2S catalytic oxidation over an NFC catalyst. Chen et al.[56] systemically investigated the influence of Na_2CO_3-impregnated NFC pore structure on H_2S-selective catalytic oxidation at low temperature. Different from the N dope-active carbon material, the sulfur saturation capacity of the catalysts depends only on pore structure and is independent of nitrogen functional groups. The H_2S oxidation products of overly impregnated NFC are mainly elemental sulfur and small amounts of sulfuric acid. More sulfuric acid forms in smaller micropores (d < 0.7 nm) because of the high surface energy and space limitations. H_2S is oxidized predominantly into elemental sulfur in larger pores (d > 0.7 nm), where most of the Na_2CO_3 is deposited. Because elemental sulfur is the dominant product and is deposited mostly in large pores, sulfur saturation capacity is determined mainly by large pore volume. The detailed catalytic process schematic is exhibited in Figure 4. In addition, the catalytic performances of carbon-based catalysts are summarized in Table 2.

2.2. Metal Oxide-Based Catalysts. Metal oxide-based catalysts are those most employed and studied in the continuous process of H_2S-selective catalytic oxidation. The main feature of metal oxide-based catalysts is that they can perform steadily only at certain ratios of $H_2S/O_2/H_2O$. Moreover, the H_2S concentration and GHSV are usually much higher than those for carbon-based catalysts.

2.2.1. Metal Oxide Catalysts. The reaction rates of H_2S-selective catalytic oxidation reaction and Claus reaction over various metal oxides (MgO, Al_2O_3, TiO_2, Bi_2O_3, Sb_6O_{13}, V_2O_5, Cr_2O_3, Mn_2O_3, Fe_2O_3, CoO, CuO, and so on)[57] have been investigated and collected in Table 3. A series of H_2S-selective oxidation activities by oxygen ($H_2S/O_2 = 0.5$) can be represented as V_2O_5 > Mn_2O_3 > CoO > TiO_2 > Fe_2O_3 > Bi_2O_3 > Sb_6O_{13} > CuO > Al_2O_3 = MgO = Cr_2O_3. Among these, V_2O_5, MgO, and Mn_2O_3 are considered the most selective catalysts.

Notably, iron- and vanadium-based catalysts have induced a larger amount of research effort in past decades compared with other metal oxide-based catalysts. Iron oxide has relatively high activity for H_2S oxidation,[58,59] but its sulfur selectivity is quite low because of the excess oxygen requirement. Fortunately, a number of methods have been established to modify iron oxide catalysts to obtain more selective and stable catalysts, particularly by incorporating a second metal element into the iron oxide

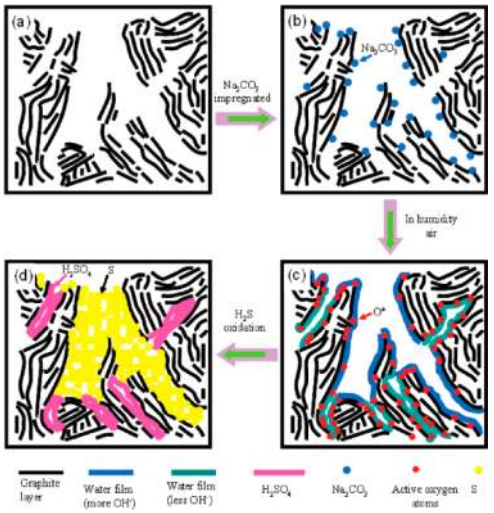

Figure 4. Schematic representation of H_2S oxidation and sulfur species deposition in the pores: (a) original NFC, (b) impregnated NFC, and (c, d) NFC before and after desulfurization.[56] Figure reproduced from ref 56 with permission from the American Chemical Society, Copyright 2010.

structure.[59−63] According to the literature,[60] the selectivity and catalytic performance of an iron oxide catalyst can be improved by incorporating cerium into the catalyst structure. In particular, a 2Fe-2Ce catalyst with an equimolar ratio of Ce to Fe exhibits extremely high catalytic activity and sulfur selectivity at 250 °C. H_2S conversion and sulfur selectivity are as high as 99% under conditions of GHSV = 21 000 h^{-1}, 1% H_2S, and O_2/H_2S = 0.5. The high catalytic and sulfur selectivity is due mainly to improved redox ability by cerium and the oxygen offered by the cerium lattice, and iron species are existed mainly in the form of Fe^{3+} clusters and a-Fe_2O_3 crystallites. In addition, the formation of FeS_2 is responsible for the catalyst deactivation. Moreover, iron oxide catalysts have excellent catalytic activity over a wide temperature range when the catalyst is modified with antimony and tin.[61] Iron-rich catalysts (with a Fe/Sb atomic ratio > 1) have better activity and selectivity, and 100% sulfur yield has been obtained over a temperature range of 210−280 °C for a catalyst with Fe/Sb = 3/2 and H_2S/O_2 = 10 as a result of the coexistence and interaction of $FeSbO_4$ with Fe_2O_3. The Fe/Sn = 1 catalyst exhibits the best catalytic performance, and a 100% sulfur yield was obtained over a temperature range of 240−300 °C. The excellent catalytic performance of Sb- and Sn-modified mixed-metal oxide catalysts can be explained by a "remote control" mechanism. In this mechanism, iron oxide sites produce mobile oxygen species, which migrate to the surface of $FeSbO_4$ or SnO_2 to create new active sites and improve catalytic activity. However, the GHSV for the reaction is unclear. In contrast, a Nb-modified mesoporous Nb/Fe mixed-oxide catalyst[62] exhibits outstanding catalytic performance (99% H_2S conversion and sulfur yields at 220 °C) at a relatively higher GHSV (30 000 h^{-1}), which can be ascribed to the high surface area and the relatively thick pore walls of mesoporous Nb/Fe mixed oxide.

Nickel, chromium,[59] and molybdenum[63] are also used to modify iron oxide ($Ni_3Fe_4(PO_4)_6$, mixed Fe−Cr oxide with Cr/Fe = 0.5 and $Fe_2(MoO_4)_3$); however, all catalysts exhibit rather poor catalytic activities in the reaction temperature range. The H_2S conversion rates of $Ni_3Fe_4(PO_4)_6$ and mixed Fe−Cr oxide at 230 °C with H_2S/O_2 = 1 are only 76% and 35%, respectively. However, the Mo-modified catalyst has a much lower catalytic

DOI: 10.1021/cs501476p
ACS Catal. 2015, 5, 1053−1067

Table 2. Different Carbon -Based Catalysts Used in Selective Oxidation of H_2S to Elemental Sulfur

	reaction parameters					
	cat.	GHSV, h^{-1}	temp, °C	RH, %	sulfur capacity; g H_2S/g	sulfur yield, %	ref
H_2S, 3000 ppm	wood-based active carbon	2100	25	80	0.298		20
H_2S, 1000 ppm	Na_2CO_3-modified carbon		30	80	0.42		35, 36
H_2S, 3000 ppm; O_2, 3000 ppm	Mn/actived carbon	3000	180		0.142		21
H_2S, 1000 ppm	nitrogen-rich mesoporous carbon		30	80	2.77		44
H_2S 2000 ppm, O_2 3200 ppm	Ni_2S-modified CNTs		60	30	1.8		31
H_2S, 1000 ppm; O_2, 1%	Na_2CO_3-modified single-walled CNTs		30	80	1.86		48
H_2S, 1000 ppm; O_2, 2.5%	macroscopic N-CNTs	0.72−1.2 h^{-1} (WHSV)	190	80		68	49
H_2S, 10000 ppm; O_2, 1.25%	Ni−Cu modified NFC	3100	200	0		82	54
H_2S, 1000 ppm; O_2, 1%	pitch-based NFC		30	80	0.81		56

Table 3. .[57] Main Characteristics of Oxide Catalyst[a]

		reaction rate ×10^{-13} (molecules H_2S/(cm^2 s))		
oxide	S_{BET} (m^2/g)	(I)[b]	(II)[c]+ (III)[d]	(III)
MgO	92	1.32	0.54	0.54
CaO	3.3	1.50		
La_2O_3	11	3.00		
TiO_2	73	4.9	3.8	2.7
ZrO_2	48	0.59		
V_2O_5	3.2	80	384	372
Cr_2O_3	24	0.37	0.72	0.54
MoO_3	0.4	0.7		
Mn_2O_3	4.5	3.5	8.1	7.8
Fe_2O_3	5.6	0.04	13	2.6
CoO	0.16	0.3	12.9	6.8
NiO	1	0.02		
CuO	0.3	7.0	1.96	1.12
ZnO	2.0	0.02		
Al_2O_3	230	1.10	0.68	0.58
Ga_2O_3	15	0.02		
In_2O_3	25	0.2		
SiO_2	300	<0.0001		
SnO_2	15	0.01		
Sb_6O_{13}	42	0.002	4.0	1.4
Bi_2O_3	0.3	0.04	47	2.4

[a]Table reproduced from ref 57 with permission from Elsevier, Copyright 2003. [b]Means reaction 2. [c]Means reaction 5. [d]Means reaction 3.

activity than that of the other catalysts in the 220−300 °C temperature range: H_2S conversion < 20%.

Recently, a series of Fe-containing SBA-Fe_x materials were synthesized and used for H_2S-selective catalytic oxidation.[64] The existence form of iron species is depended mainly on the Si/Fe ratio (isolated Fe^{3+}species, extra framework iron oligomers, or aggregated iron oxide clusters). The H_2S conversion decreases with the rise of Fe content under the condition of H_2S/air/He = 1.2/5.0/93.8 at 200 °C (the SBA−Fe_5 can obtain 90% H_2S conversion and nearly 99% sulfur selectivity). The catalyst deactivation is mainly due to the presence of sulfate species.

Catalysts containing vanadium oxide are active for the reaction with both a stoichiometric and an excess amount of oxygen. Moreover, binary and ternary oxides are applied widely to modify vanadium-containing catalysts, among which molybdenum-, magnesium-,[65] iron-, bismuth-, chromium-, titanium-, manganese-, zirconium-,[66] and alkali metal[67,68]-modified catalysts have been researched intensively. A Fe-, Bi-, Cr-, Ti-, Mn-, and Zr-modified catalyst test was performed under conditions of H_2S/O_2 = 5/2.5, GHSV = 94 000 h^{-1} at different temperatures in the presence of 30% water. Only the $TiVO_x$ catalyst maintained stable activity without deactivation for 50 h (85% H_2S conversion and 90% sulfur selectivity) at the relatively lower temperature of 230 °C despite $BiVO_x$ and ZrV_2O_7 exhibiting excellent activity at the higher temperature of 250 °C, but the others deactivated eventually.

The partial transformation of $FeVO_x$, $MnVO_x$, and $CrVO_x$ to FeS_2, $VOSO_4$, and an amorphous Cr phase are the main reasons for catalyst deactivation. Moreover, it was revealed that the BiVOx catalyst with V/Bi = 0.5 presents 95% H_2S conversion and 100% sulfur selectivity under conditions of H_2S/O_2 = 0.2 at 200 °C in the absence of water. The excellent activity can be attributed to the coexistence of Bi_2S_3, $Bi_4V_6O_{21}$, and $BiVO_4$. Under the same conditions, vanadium−molybdenum with V/Mo = 5 attained the best catalytic activity, with 80% H_2S conversion and 99% sulfur selectivity due to the strong synergistic behavior between vanadium oxide and molybdenum oxide. The vanadium and molybdenum existed mainly in the form of $Mo_6V_9O_{40}$.

In the case of alkali metal (K, Na, Li, Cs)-modified catalysts,[67,68] Na was considered as the most efficient promoter to improve the catalytic activity. The existing form of vanadium species depended mainly on the Na/V ratio. Among them, a Na/V = 0.1 catalyst presented the best catalytic activity (95% H_2S conversion and 100% sulfur selectivity under the condition of H_2S/air/He = 1.2/5/93.8 at 200 °C), wherein, vanadium species existed mainly in the form of V_2O_5 and $Na_{0.33}V_2O_5$. However, the V_2O_5 species were transformed to V_4O_9 totally after the reaction. It was realized that the V^{5+}−O−V^{4+} pairs presented in V_4O_9 and $Na_{0.33}V_2O_5$ are the active phase, and the $Na_{0.33}V_2O_5$ species contributed to the catalyst stability. On the other hand, in the case of Mg-modified catalysts, the H_2S conversion for vanadium−magnesium with V/Mg = 3 is only 80%, but sulfur selectivity was 100%. However, both the catalytic activities and the maximum sulfur yields of magnesium vanadate decrease with an increase in magnesium content, when the V/Mg ratios are 2/1, 1/1, and 2/3.[69] The maximum sulfur yields obtained with MgV_2O_6, $Mg_2V_2O_7$, and $Mg_3V_2O_8$ are 88.4% (at 210 °C), 78.6% (at 260 °C), and 74.1% (at 260 °C), respectively. Moreover, vanadium cations in magnesium vanadate are major active sites.

Meanwhile, rare earth elements have electronegativities similar to that of Mg (electronegativity, 1.2). Therefore, H_2S-selective oxidation of rare earth−vanadium binary oxides ($CeVO_4$, YVO_4,

DOI: 10.1021/cs501476p
ACS Catal. 2015, 5, 1053−1067

$LaVO_4$, and $SmVO_4$)[69] has been investigated. The maximum sulfur yields obtained for YVO_4, $CeVO_4$, $LaVO_4$, and $SmVO_4$ are 91.8% (at 210 °C), 93.1% (at 230 °C), 78.8% (at 220 °C), and 83.9% (at 240 °C), respectively. All are higher than those of Mg-modified catalysts. Among them, YVO_4 possesses a significantly higher reaction rate because of a higher surface area. The improved cation reducibility of the rare earth orthovanadates is responsible for the higher sulfur yield and selectivity because the aqueous reduction potentials of the R_E^{3+} ions are approximately −2.3 V,[70] whereas the aqueous reduction potential of V^{5+} is 1.0 V.[71]

Differences in ionic radii (Mg^{2+} is 0.72 Å[72] with respect to 1−1.17 Å of R_E^{3+} ions) are the major reasons why magnesium vanadates have much lower activities compared with those of rare earth orthovanadates. Yasyerli et al.[73] also confirmed that a Ce−V mixed-oxide catalyst containing equimolar quantities of cerium and vanadium has very high catalytic activity (100% H_2S conversion and 97% sulfur selectivity) under conditions of H_2S/O_2 = 1 at 250 °C. However, it revealed that the reaction process most probably involved a redox cycle of cerium, rather than a redox cycle of vanadium. In contrast, ternary oxides have much higher catalytic performance compared with that of binary oxides because of a third species, such as Sb, introduced into the La−V structure[74] to improve catalytic performance. The synergistic effect of the mixed-metal oxides associate with the formation of $SbVO_4$ species strongly improves sulfur selectivity and sulfur yield (maximum yield increased from 88.5% for $LaVO_4$ to 100% for La−V−Sb with a V/Sb atomic ratio = 1.0). Moreover, La−V−Sb catalysts have a much wider temperature range to provide 100% sulfur yield (240−300 °C) because there is better isolation of active sites (caused by the large size of La^{3+}) and easier desorption of elemental sulfur (caused by lanthanum basicity). A similar phenomenon is observed for V/Sn/Sb ternary oxides,[75] which exhibit a 100% sulfur yield over a relatively lower temperature range (180−240 °C) as a result of improved vanadium reducibility and increased surface area.

Significantly, a MgAlVO ternary oxide derived from vanadium containing LDH materials was obtained and first applied for H_2S-selective oxidation recently.[76] As is known, layered double hydroxides (LDHs) with the general formula $Mg_{1-x}^{2+}Al_x^{3+}(OH)_2$ $(anion_{x/n}^{n-})\cdot yH_2O$, are anionic clay materials.[77] LDHs and their derivatives were investigated intensively as catalysts and catalyst supports because their acid/base properties can be tuned easily[78] and their composition can be changed.[79] It was observed that the vanadium species existed mainly in the form of isolated V^{5+} in distorted $[VO_4]$, $Mg_3V_2O_8$, and VO^{2+} in MgAlVO catalyst. This catalyst exhibits a maximum 95% sulfur yield at a relatively high space velocity (GHSV = 24 000 h^{-1}) at 180 °C. It is believed that the basic sites play a crucial role in the reaction. The catalytic mechanism was proposed that H_2S is first adsorbed on the Mg−O−Mg band of MgO (moderate basic sites), forming S^{2-} and H_2O, then S^{2-} is oxidized to S_n by V^{5+}, which forms oxygen vacancies in the process. Finally, V^{4+} is oxidized to V^{5+} by O_2, and O^{2-} is incorporated into the oxygen vacancies. Deactivation of this catalyst was due mainly to a decrease in the number of moderate basic sites.

2.2.2. Oxide-Supported Catalysts. The choice of an appropriate support is an important issue. Use of a suitable support provides some unique advantages. A good interaction between the active phase and the support can prevent significant sintering of the active phase. However, the use of a support can also cause some difficulties. Catalytic reactions that proceed on the bare part of the support surface may affect selectivity negatively. In addition, an interaction between the active phase and the support can lead to a new phase with undesired catalytic properties, or it can cause deactivation.[80]

SiO_2, Al_2O_3, and TiO_2 are the three main kinds of catalyst supports that are applied widely. SiO_2, unlike Al_2O_3, MgO, or Fe_2O_3, cannot be sulfated easily by heating with H_2S or SO_2 and excess oxygen. Many SiO_2-supported catalysts have been synthesized and investigated intensively. Chun et al.[81] prepared a serial TiO_2/SiO_2 catalyst, and the 30 wt % TiO_2/SiO_2 showed the best catalytic activity with 94% H_2S conversion and 98% sulfur selectivity under conditions of H_2S/O_2 = 5/2.5 at 275 °C and GHSV = 3000 h^{-1}. However, H_2S conversion and sulfur selectivity decreased sharply (80% H_2S conversion and 90% sulfur selectivity) when 10% water vapor was introduced into the stream, indicating that TiO_2 is easily poisoned by water vapor. An increase in the O_2/H_2S ratio from 0.5 to 4 influenced the H_2S conversion rate slightly, but sulfur selectivity was decreased remarkably. A similar tendency was observed for a CrO_x/SiO_2 catalyst[58] and a VO_x/SiO_2 catalyst.[66,82,83] The reaction evaluation after K_2O and B_2O_3 doping of TiO_2/SiO_2 confirmed that selective oxidation of H_2S occurred on acidic sites and that the reverse Claus reaction proceeded on basic sites. Deactivation of the catalyst was mainly due to deposition of elemental sulfur rather than sulfation and sulfidation of TiO_2; however, under the same reaction conditions, a 10 wt % $CrOx/SiO_2$ catalyst showed poor H_2S conversion and sulfur selectivity (84% and 86%, respectively) at a relatively higher temperature of 325 °C. Conversion and selectivity were much lower than those of the TiO_2/SiO_2 catalyst and unsupported Cr amorphous catalysts. Notably, a 10 wt % CrO_x/SiO_2 catalyst exhibits strong resistance against water, even when the water content is as high as 20%, if the reaction temperature is >300 °C. On the other hand, the catalytic activity of a VO_x/SiO_2 catalyst increases with increased vanadium content. According to Bars et al., 10 wt % V loading is the theoretical coverage of a vanadium oxide monolayer over SiO_2 (300 m^2/g) in the form of VO_4. Therefore, a 30 wt % VO_x/SiO_2 catalyst can attain catalytic performance as high as 90% H_2S conversion and 92% sulfur selectivity at 225 °C, even in the presence of 30% water under the same condition.

In contrast to a TiO_2/SiO_2 catalyst, deactivation of the catalyst is due mainly to reoxidation by the O_2 gas phase rather than the formation of $VOSO_4$ species, which proceeds at a much slower rate than the H_2S reduction step. The increase of the reaction temperature can efficiently resist to the catalyst deactivation. As the temperature increases, the rate of reoxidation increases at a faster rate than reduction, which prevents the reversible reduction of the catalyst. Fe_2O_3/SiO_2 catalysts[80] also exhibit excellent catalytic performance with 97% sulfur selectivity and 94% sulfur yield at 240 °C in the presence of 30% water under the condition of H_2S/O_2 = 1/5. The high catalytic activity can be ascribed to the fact that SiO_2 can significantly stabilize the formed iron(II) sulfate species. Otherwise, the sintering of the species can result in the loss of active surface, therefore causing the decrease in the catalytic activity. However, the sulfur selectivity decreased sharply with the further rise of reaction temperature, which probably was due to the reaction between the oxygen and sulfur radical on SiO_2 support. Moreover, the formation of FeS_2 species can also cause the decrease in the sulfur selectivity. Fortunately, the incorporation of sodium can improve the sulfur selectivity of Fe_2O_3/SiO_2 greatly,[84] because adding basic sodium affects SiO_2 by destroying the acid sites and suppressing formation of sulfur radicals. Simultaneously, an increase in the calcination temperature can enhance the stability of the catalyst

DOI: 10.1021/cs501476p
ACS Catal. 2015, 5, 1053−1067

in the sulfidation of the active component (Fe_2O_3) into the FeS_2 phase,[85] whereas it decreases catalytic activity due to agglomeration of iron oxide particles and a decrease in the surface active site concentration.

The most widely used catalyst for H_2S selective catalytic oxidation is iron oxide/chromium oxide supported on *a*-alumina with a relatively low specific surface area. Chromium oxide is added to decrease the rate of catalyst deactivation.[86] This catalyst is also resistant to a large amount of water. However, a practical large-scale experiment revealed that sulfur selectivity is rather poor at only 80−82%. Moreover, chromium is toxic, and stability of the catalyst depends strongly on the chromium oxide distribution in the iron oxide phase, which makes large-scale production difficult. In this situation, various metal oxides (Fe, Co, Mn, and V), supported on spherical (*a*, *r*, *r* + *x*) Al_2O_3, were prepared and evaluated.[87] The sulfur selectivity of Fe_2O_3/*r*-Al_2O_3 catalysts is independent on Fe content and is maintained at 99% at 250−300 °C under the condition of stoichiometric H_2S/O_2 mixtures (C_{H_2S} = 15−20 vol %). In contrast, under the same condition, the H_2S conversion increases with elevations in Fe content and reaction temperature. The highest H_2S conversion for a 1.3% Fe-containing catalyst is 90% at 300 °C. The improved sulfur selectivity is explained by the fact that the bond energy of surface oxygen in catalyst systems increases greatly. This decreases oxygen reactivity, which leads to a predominance of H_2S-selective catalytic oxidation and decreased SO_2 yield. However, H_2S conversion is extraordinarily dependent on Co content for Co−O/*r*-Al_2O_3 catalyst because of interactions between the active components and the support. In addition, the active Co species existed mainly in the form of Co_3O_4 and $CoAl_2O_3$, whose ratio depends on the active component concentration and calcination temperature.

When the *r*-Al_2O_3 support was replaced by *a*-Al_2O_3 and (*r* + *x*)-Al_2O_3, the catalytic activity decreased greatly. Nevertheless, a Mn oxide-supported catalyst exhibits a rather poor H_2S conversion rate of only 40% at 300 °C. However, a vanadium oxide-supported catalyst has specific catalytic features because it exhibits a high H_2S conversion rate of 92% at 200 °C, whereas the H_2S conversion rate at 200 °C is only 20% for the other metal oxide catalysts examined, but it achieves its maximum value only at temperatures >300 °C. However, the H_2S conversion decreases with a rise in the potassium content[88] when potassium was added as a promoter, which is due mainly to the poisoning effect of alkaline cations on the hydrocarbon activation centers and formation of less active $VOSO_4$.[89] The highest sulfur yield can be obtained (almost 80%) at 250 °C with a V/K = 0.2 under the condition of H_2S/O_2/He = 1/0.87/98.3. The addition of small amounts of K makes the crystallinity and oxidation state of vanadium increase, which is more active for the H_2S-selective oxidation.

More importantly, TiO_2-supported catalysts present reasonable catalytic performance in the presence of water. For example, a 10 wt % VO_x/TiO_2 catalyst exhibits an 84% H_2S conversion rate and 95% sulfur selectivity, even in the presence of 30% water vapor at 230 °C.[66] Moreover, the multimetallic oxide V−Fe−Cr−Mo−O_x/TiO_2 catalyst exhibits an almost 90% H_2S conversion rate, which is higher than that of VO_x/TiO_2 under identical conditions. It revealed that TiO_2 promotes the reoxidation step of reduced vanadium oxide through a surface oxide−support interaction between TiO_2 and V_2O_5 at surface redox sites, which improves the catalytic performance and inhibits catalyst deactivation compared with that of a VO_x/SiO_2 catalyst. The incorporation of Fe improves the redox property.

Other metal oxides, such as MgO and ZrO_2, have also been investigated as catalyst supports. Van den Brink et al.[80] prepared different catalysts by loading Fe on various supports (SiO_2, Al_2O_3, MgO, TiO_2, and ZrO_2), suggesting that all catalysts (except MgO-supported catalysts) have much better catalytic activity at relatively lower temperatures compared with that of a commercial Fe_2O_3−Cr_2O_3/Al_2O_3 catalyst under conditions of 1% H_2S, 5% O_2, and 30% H_2O. The catalytic performances of various supported catalysts are shown in Figure 5. It can be

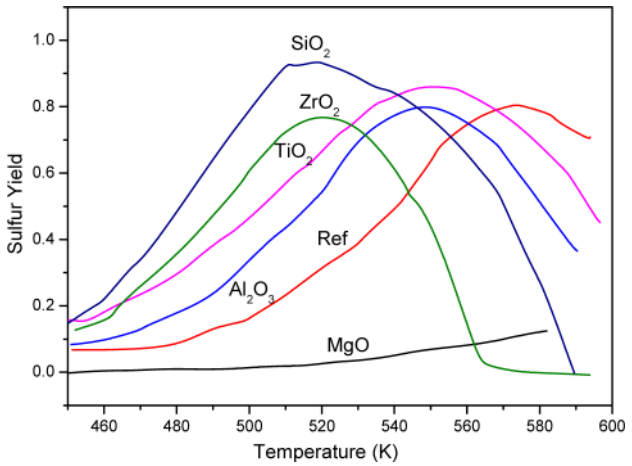

Figure 5. The catalytic performances of various supported catalysts.[80] Figure reproduced from ref 80 with permission from Elsevier, Copyright 1993.

observed that Al_2O_3- and TiO_2-supported catalysts have similar tendencies. Both obtain the best sulfur yield at 277 °C, which is due to the larger specific surface area of the support. SiO_2- and ZrO_2-supported catalysts have their best sulfur yields at a much lower temperature of ∼240 °C; however, MgO-supported catalysts exhibit even poorer activity, which is due mainly to the reaction between MgO and iron(II) sulfate.

2.2.3. Clay-Supported Catalysts. Clay is nanoscopic in size, anisotropic in shape, apparently nontoxic, low in cost, and very abundant; however, efficient use of clays is limited by their low porosity and poor thermal stability. Fortunately, the pillaring process has been developed and is widely used to modify clay. Pillared interlayered clays (PILCs) are two-dimensional zeolite-like materials prepared by exchanging the charge-compensating cations between clay layers with large inorganic cations, which are polymeric or oligomeric hydroxy metal cations, formed by hydrolysis of metal oxides or metal salts. This process provides porosity and thermal stability. Upon heating, the metal hydroxy cations undergo dehydration and dehydroxylation, forming stable metal oxide clusters that act as pillars to maintain separation between the silicate layers and create an interlayer space of molecular dimensions. PILCs can be tailored to particular applications by varying the size and separation of the pillars as well as their composition. Many metal oxides, such as TiO_2, ZrO_2, and Fe_2O_3, can be utilized as pillars. For example, Bineesh et al.[90,91] investigated the catalytic performance of vanadium-doped delaminated zirconium-pillared montmorillonite clay for selective catalytic oxidation of H_2S at 220−300 °C, GHSV = 10 000 h^{-1} and H_2S/O_2/He = 5/2.5/92.5. A 6 wt % vanadium-loaded catalyst exhibited the highest catalytic activity at 300 °C (95% sulfur yield), which was attributed to the high

DOI: 10.1021/cs501476p
ACS Catal. 2015, 5, 1053−1067

Table 4. Different Metal Oxide Catalysts Used in Selective Oxidation of H_2S to Elemental Sulfur

	reaction parameters									
feed	catalyst	O_2/H_2S	GHSV, h^{-1}	temp, °C	conversion, %	selectivity, %	yield, %	active phase chemical state	catalyst deactivation	ref
1% H_2S balance with helium	2Fe−2Ce	0.5	21 000	250	99	99	98	Fe^{3+} clusters and a-Fe_2O_3	formation of FeS_2	60
$H_2S/O_2/He$ = 1/5/94	Fe/Sb = 3/2	5		210−280	100	100	100	$FeSbO_4$, Fe_2O_3		61
	mesoporous Nb/Fe mixed oxide	0.5	30 000	220	99	99	98			62
H_2S/air/He = 1.2/5.0/93.8	SBA-Fe5	4.2 (air)		200	90	99	89	isolated Fe^{3+}species	formation of sulfate species	64
H_2S/O_2 = 5/2.5 with 30% water	$TiVO_x$	0.5	94 000	230	85	90	77			66
$H_2S/O_2/N_2$ = 1/5/94	V/Mo = 5	5		200	80	99	79	$Mo_6V_9O_{40}$		65
$H_2S/O_2/N_2$ = 1/5/94	YVO_4	5		210			92	V^{5+}		69
H_2S/air/H_2 = 1.2/5/9.8	Na/V = 0.1	4.2 (air)		200	95	100	95	V^{5+}−O−V^{4+} pairs		67, 68
H_2S/O_2 = 1/2.5 with 30% water	Fe_2O_3/SiC	2.5	3 000	250	100	95	95	$Fe_2O_3{\cdot}xSO_3$		103
$H_2S/O_2/He$ = 5/2.5/92.5	6%V_2O_5/Zr-PILC	0.5	10 000	300	98	95	93	monomeric and polymeric vanadium	formation of crystalline V_2O_5	90, 91
$H_2S/O_2/He$ = 5/2.5/92.5	5%V_2O_5/TiO_2−PILC	0.5	10 000	220	100	97	97	monomeric and polymeric vanadium	formation of crystalline V_2O_5	92, 93
$H_2S/O_2/He$ = 5/2.5/92.5	7%V_2O_5/Fe_2O_3−PILC	0.5	10 000	300	99	96	95	monomeric and polymeric vanadium	formation of crystalline V_2O_5	94, 95
H_2S/O_2N_2 = 0.5/0.25/99.25	7%Fe/Al-Lap	0.5	7 000	180	98	97	95	isolated Fe^{3+}	$Fe_2(SO_4)_3$	96
H_2S/O_2N_2 = 0.5/0.25/99.25	5%V_2O_5/CeO_2−Lap	0.5	7 000	180	99	99	98	isolated V^{5+}	slower oxidation rate	97

DOI: 10.1021/cs501476p
ACS Catal. 2015, 5, 1053−1067

dispersion of vanadium in the form of monomeric and polymeric species. Furthermore, an increase in Brønsted acidity also contributes to catalytic performance. Contrary to the oxide support and modified vanadium catalysts, the presence of crystalline V_2O_5 decreases the catalytic activity. However, catalytic activity decreased significantly (85% sulfur yield at 280 °C) in the presence of 20 vol % water. This result may be due to competition between H_2S and water vapor for the same active catalyst sites. Although TiO_2[92,93] was used as a pillar, a 5% V_2O_5/TiO_2−PILC catalyst obtained the best catalytic performance at 220 °C (almost 97% sulfur yield) under the same water-free conditions; however, the catalyst reacted differently with an increase in reaction temperature compared with that of V_2O_5/Zr-PILC, which activity decreased with an increase in temperature. More importantly, sulfur selectivity was maintained at 98% in the presence of 20% water, whereas the H_2S conversion rate decreased slightly from 99% to 98% at 220 °C. A similar phenomenon is observed for the V_2O_5/Fe_2O_3−PILC catalyst,[94,95] which attains a maximum sulfur yield of 95% under water-free conditions at 280 °C and 90% in the presence of 20% water.

A new method was developed to modify clay in the presence of surfactants, which provides a more enriched mesoporous structure and high thermal stability. Zhang et al.[96] prepared catalysts that were iron oxide-supported on alumina-intercalated Laponite clay. They demonstrated that the iron species existed mainly in the form of isolated Fe^{3+}. A 7% Fe-loaded catalyst showed the best catalytic performance at relatively low temperature (180 °C) with 95% sulfur yield and excellent stability. However, deactivation of the catalyst occurred due to the formation of $Fe_2(SO_4)_3$ species. The surface of catalysts composed of V_2O_5[97] supported on CeO_2-intercalated Laponite clay contains abundant chemically adsorbed oxygen vacancies, which benefits this reaction. Sulfur yield can be as high as 97% at 180 °C. Deactivation of the catalyst is due mainly to the slower oxidation rate of the catalyst active phases by oxygen compared with the H_2S reduction rate. Ce^{3+} can resist deactivation of the catalyst significantly.

In addition, a mesoporous zirconium phosphate species was prepared and applied to support the anadium active species.[98] It was demonstrated that the catalysts presented high and stable catalytic performance when vanadium species existed mainly in the V_2O_5 crystallite form because it can be transformed to V_4O_9 species containing V^{5+}−O−V^{4+} active pairs in the reaction. A 98% H_2S conversion can be attained for 12 V-MZP catalyst under the condition of H_2S/air/He = 1.2/5.0/93.8 at 200 °C. Furthermore, the vanadium species can be partially incorporated into the structure of the gallery of zirconium phosphate material with or without the presence of TEOS,[99,100] which strongly affects the dispersion of vanadium species. Therefore, the catalyst prepared with TEOS exhibited relatively higher catalytic activity due to the higher accessible V-surface concentration. Particularly, a structured catalyst was obtained starting with honeycomb cordierite monoliths and a commercial ceria/zirconia based washcoat, to which the vanadium active species was added.[101,102] The 19% V_2O_5 loaded catalyst can present 92% H_2S conversion at GHSV = 18 000 h^{-1} with stoichiometric H_2S/O_2. However, the initial H_2S concentration is rather low, only 500 ppm.

Meanwhile, the other materials, such as SiC with a well-defined meso- and macroporous network, can also be employed as a catalyst support. For Fe_2O_3/SiC,[103] it can present 100% H_2S conversion and 95% sulfur selectivity under the condition of H_2S/O_2 = 1/2.5, GHSV = 3000 h^{-1} in the presence of 30% H_2O at 250 °C. Significantly, sulfur was incorporated into the iron oxide lattice. Fe_2O_3 transformed into an Fe^{III} intermediate ($Fe_2O_3{\cdot}xSO_3$ ($x < 2$)) in the reaction process, which was considered as the true active phase.

The catalytic performances of metal oxide-based catalysts are collected in Table 4, and the advantages and drawbacks of all catalysts are compared and listed in Table 5.

Table 5. Detailed Information of Catalysts

catalyst	advantage	disadvantage
carbon	high adsorption capacity	mainly discontinuous process
	low operation temperature	low H_2S concentration
	thermodynamic stability	produce poisoned by product (COS, CS_2)
metal oxide and oxide supported	high catalytic performance; can be prepared easily	perform steadily only at certain ratios of $H_2S/O_2/H_2O$
	relatively high H_2S concentration	relatively high reaction temperatures (higher than 200 °C)
clay-supported	eco-friend material	new developed catalyst
	can be easily tailored to particular applications	
	high catalytic performance; excellent regenerability	

3. CATALYTIC AND DEACTIVATION MECHANISMS

3.1. Catalytic Mechanisms for Carbon-Based Catalysts.

The catalytic mechanisms for carbon materials have been investigated. In general, two types of catalytic mechanisms have been proposed by different researchers.[6]

Mars−van Krevelen mechanism:

$$O_2(g) + 2X \rightarrow 2O{-}X$$

$$O{-}X + H_2S \rightarrow S{-}X + H_2O(g)$$

Langmuir−Hinshelwood mechanism:

$$\frac{1}{2}O_2(g) + X \rightarrow O{-}X$$

$$H_2S(g) + X \rightarrow H_2S{-}X$$

$$H_2S{-}X + O{-}X \rightarrow H_2O(g) + S{-}X + X$$

The last step is considered the rate-determining step by Ghosh and Tollefson;[104] however, there is some disagreement about H_2S adsorption: Ghosh and Tollefson claim that H_2S is physiosorbed, whereas Steijns et al.[105] insist that H_2S adsorption is dissociative. Zhenglu et al.[106] reported that the catalytic mechanism for carbon material is best represented by the Mars−van Krevelen mechanism. Yan et al.[107] confirmed that physiosorbed H_2S dissociates to HS^- and that water plays a key role in the reaction, which generally includes physical adsorption, chemical adsorption, and oxidation steps. Therefore, the catalytic mechanism for unmodified carbon material can be revised as the following:[107,19]

Physical adsorption step: H_2S is first adsorbed on the carbon surface, then H_2S is dissolved in a water film and dissociates in an adsorbed state in the water film.

$$H_2S(g) \rightarrow H_2S(ads)$$

$$H_2S(ads) \rightarrow H_2S(ads - liq)$$

$$H_2S(ads - liq) \rightarrow HS^-(ads) + H^+$$

DOI: 10.1021/cs501476p
ACS Catal. 2015, 5, 1053−1067

Oxidation step: the adsorbed H_2S reacts with oxygen to produce elemental sulfur or sulfur dioxide, and SO_2 is further oxidized to H_2SO_4 in the presence of water.

$$HS^- + O^*(ads) \rightarrow S(ads) + OH^-$$

$$HS^- + 3O^*(ads) \rightarrow SO_2(ads) + OH^-$$

$$SO_2(ads) + O^*(ads) + H_2O(ads) \rightarrow H_2SO_4(ads)$$

$$H^+ + OH^- \rightarrow H_2O$$

In contrast, the reaction mechanism is remarkably different when the carbon is modified by different species, such as KOH, Na_2CO_3, and NaOH. The catalytic mechanism for KOH-modified carbon material changes with respect to the surface pH.[108]

(1) When the carbon surface pH is >7.0, chemisorption dominates the beginning of H_2S adsorption.

$$H_2S(g) + KOH(q) - C \rightarrow KHS(q) + H_2O$$

$$KHS(q) \leftrightarrow K^+(q) + HS^-(q)$$

$$HS^-(q) \leftrightarrow HS^-(ads)$$

$$2xHS^-(ads) + xO^*(ads) \rightarrow 2S_x(ads) + xH_2O$$

(2) When the carbon surface pH is 4.5−7.0, HS^- ion concentrations are low, and physical adsorption becomes important at the intermediate stage of H_2S adsorption.

$$H_2S(g) + H_2O(q) - C \rightarrow HS^-(q) + H_3O^+$$

$$HS^-(ads) + 3O^*(ads) \rightarrow SO_2(ads) + OH^-$$

$$SO_2(ads) + O^*(ads) \rightarrow SO_3(ads)$$

$$SO_3(ads) + H_2O(ads) \rightarrow H_2SO_4(ads)$$

(3) When the carbon surface pH is <4.5, physical adsorption dominates the process.

$$H_2S(g) \rightarrow H_2S(ads)$$

$$H_2S(ads) + H_2SO_4(ads) \rightarrow S_x(ads) + xH_2O$$

$$H_2S(ads) + 3H_2SO_4(ads) \rightarrow 4H_2SO_3(ads)$$

The catalytic mechanism for Na_2CO_3-modified carbon material is represented as the following:[56]

$$H_2S + H_2O \rightarrow HS^- + H_3O^+$$

$$H_2S + CO_3^{2-} \rightarrow HS^- + HCO_3^-$$

$$H_2S + HCO_3^- \rightarrow HS^- + H_2CO_3$$

$$C-O^* + HS^- \rightarrow C_f + S^* + OH^-$$

$$xS^* \rightarrow S_x$$

$$S^* + O_2 \rightarrow SO_2$$

$$SO_2 + 0.5O_2 + H_2O \rightarrow SO_4^{2-} + 2H^+$$

C_f, C−O*, S*, and S_x represent carbon active sites, adissociatively adsorbed oxygen at carbon sites, sulfur radicals (or small sulfur chains), and sulfur polymers (or elemental sulfur), respectively.

A remarkably different catalytic mechanism is presented for NaOH-modified carbon material:[16]

$$NaOH + H_2S \rightarrow NaHS + H_2O$$

$$2NaOH + H_2S \rightarrow Na_2S + H_2O$$

$$NaHS + 0.5O_2 \rightarrow S + NaOH$$

$$Na_2S + 0.5O_2 + H_2O \rightarrow S + 2NaOH$$

$$2NaOH + H_2SO_4 \rightarrow Na_2SO_4 + 2H_2O$$

A radical mechanism has also been proposed because H_2S can dissolve to different radicals, such as HS_x, O_2, H_2S, and S_x[109,110] during the reaction, which can be intermediated by numerous steps leading to H_2S oxidation. The mechanism is complex, but it certainly involves radicals. Therefore, the H_2S oxidation reaction mechanism may be different according to the nature of the catalyst, but the radical mechanism can reasonably explain several experimental observations.

3.2. Catalytic Mechanism for Metal Oxide-Based Catalysts. The so-called Mars−van Krevelen or redox mechanism is widely applied for selective oxidation reactions of metal-oxide catalysts and involves two steps:[111]

1. A reaction between the catalyst in an oxidized form (Cat-O) and the reactant, in which the oxide becomes reduced: Cat-O + R = RO + Cat
2. The reduced catalyst (Cat) becomes reoxidized by gaseous oxygen:

2Cat + O_2 = 2Cat-O. This process cannot reach a steady-state until the rates of the two steps are consistent.

Boreskov et al.[57] further suggested that the catalytic oxidation reactions proceed on solid catalysts via two types of mechanisms: (1) a stepwise mechanism with alternating oxidation−reduction of the catalyst surface by the reactants and (2) a concerted mechanism, in which oxygen interacts with the catalyst, and the reaction products form simultaneously in the presence of both reagents only. According to Boreskov, a stepwise mechanism is implied when the reaction rate is kept consistent, both in the pulse reaction using pulses containing the reactant mixture and that using pulses containing each reactant. The so-called concerted mechanism occurs in the opposite case. Vanadium oxide catalysts follow this stepwise, as confirmed by Zhang et al.[76]

3.3. Catalyst Deactivation Mechanisms. The catalyst deactivation mechanism differs for various catalysts. In general, carbon catalyst deactivation is mainly due to pore blockage by elemental sulfur or a decrease in water−film pH because carbon plays a dual role in the reaction: it catalyzes and stores the elemental sulfur produced. However, other factors are involved for metal oxide- and clay-based catalysts, and the catalyst deactivation mechanism is remarkably different, depending on the various catalysts. The catalyst deactivation mechanism can be summarized as follows:

(1) For iron-based catalysts, the formation of less active phases,[60,64,96] such as FeS_2 and iron sulfate species, is the main reason for catalyst deactivation. However, Ti sulfate species are active during the reaction. Thus, TiO_2-based catalyst deactivation is mainly due to deposition of elemental sulfur.[81]

(2) Vanadium-based catalyst deactivation is caused primarily by the slower oxidation rate of V^{4+} by oxygen compared with the reduction rate of V^{5+} by H_2S.[82,83,97] Otherwise, the formation of $VOSO_4$[65] and crystalline V_2O_5[90−94] also

DOI: 10.1021/cs501476p
ACS Catal. 2015, 5, 1053−1067

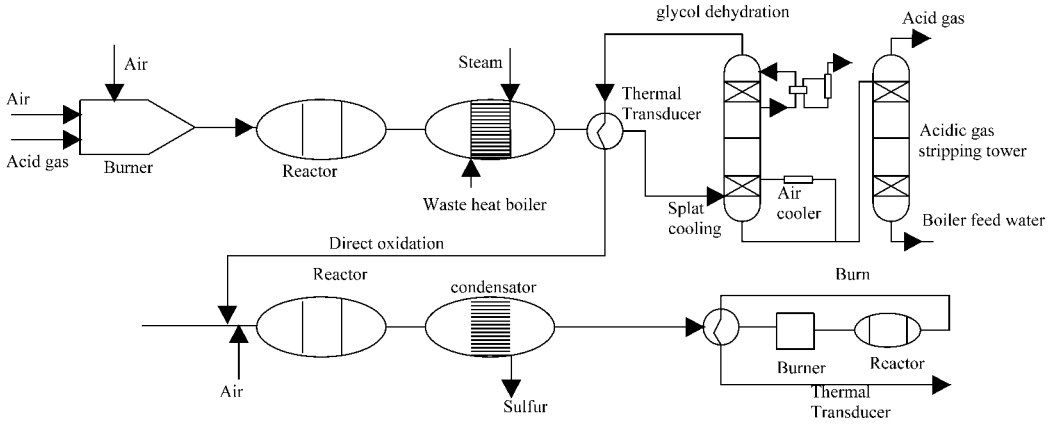

Figure 6. Flow diagram of MODOP process.

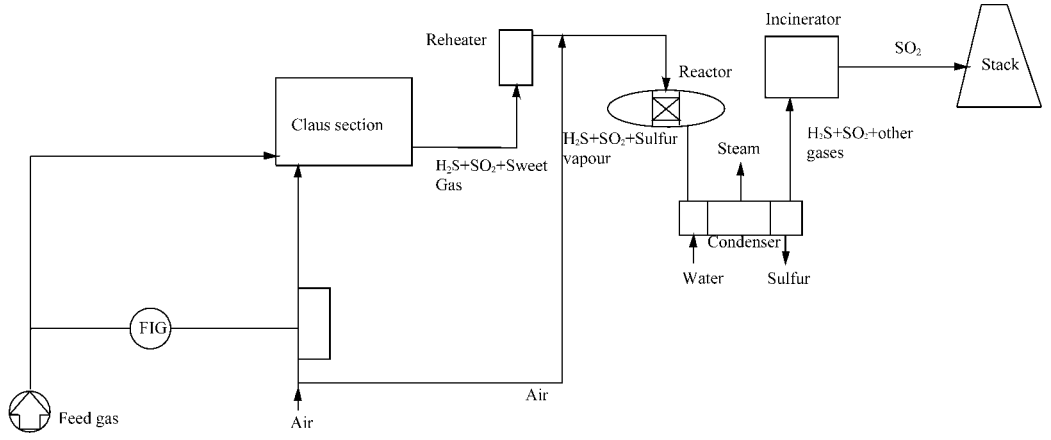

Figure 7. Schematics of super-Claus-99 process.

contributes to the catalyst deactivation. However, for MgAlVO catalyst derived from LDH materials, the catalyst deactivation is attributed mainly to a decrease in the number of moderately basic sites.[76]

3. CURRENTLY USED PROCESSES BASED ON H_2S-SELECTIVE OXIDATION

A Claus tail-gas treatment process preferably should (1) be easy to operate and flexible, (2) generate no secondary air/water pollution or waste, and (3) deliver a high degree of desulfurization over a wide range of operating conditions.[10]

4.1. Mobil Direct Oxidation Process (MODOP). MODOP was developed by a German company (Mobil-AG) and can be applied to other H_2S-containing processes. Figure 6 presents the flow diagram of MODOP process. This process consists of three parts: hydrogenation of the tail gas, dehydration of the gas, and selective catalytic oxidation.

The Claus tail gas is first reduced by H_2 in the presence of a suitable catalyst. Sulfur-containing compounds are transformed to H_2S during this step. A TiO_2-based catalyst is applied predominantly in H_2S selective catalytic oxidation part of MODOP, which is deactivated sharply in the presence of water. Therefore, the H_2S-containing gas must pass through a thermal insulation cold tower and a sour water stripping tower (mainly glycol) for dehydration. Finally, the gas is passed through a selective catalytic reactor to yield elemental sulfur. The sulfur recovery efficiencies can be as high as 99.5%.

4.2. Super-Claus Process. Development of the super-Claus process[112,113] started in 1984. The first commercial super-Claus plant began in 1988 at a Wintershall AG Barnstorf natural gas plant in West Germany. The second plant came online in February 1989 at the Netherland Refinery Company (Nerefco), and the third super-Claus plant was commissioned at Kainan Petroleum Refinery Company, Wakayama, Japan.[114] Fe_2O_3–Cr_2O_3/Al_2O_3 is a first-generation catalyst for H_2S selective catalytic oxidation in the super-Claus process. As mentioned above, this catalyst is resistant in up to 30% water. Therefore, water does not need to be removed in-stream; however, the sulfur yield is rather poor (80%), and the inlet temperature is restricted to 240–250 °C. Therefore, Fe_2O_3/SiO_2 was applied as the second-generation catalyst because of high catalytic activity, high specific surface area, and poor Claus catalytic activity. Furthermore, inlet temperature can be decreased significantly to 200 °C. A third generation catalyst is promoted with Na_2O, which decreases SO_2 formation, especially at the higher temperature in the bottom of the catalyst bed. A fourth-generation catalyst contains zinc as a promoter, which further reduces SO_2 formation at higher temperatures.[115]

The super-Claus process is used currently to treat H_2S concentrations < 2 vol %.

4.2.1. Super-Claus-99 Process. Figure 7 shows the schematics of the super-Claus-99 process. Contrary to the traditional Claus process ($H_2S/SO_2 = 2$), the H_2S concentration in the gas leaving the second Claus reactor stage is kept between 0.8 to 1.5% (volume). Therefore, the Claus reaction occurred at the thermal

DOI: 10.1021/cs501476p
ACS Catal. 2015, 5, 1053–1067

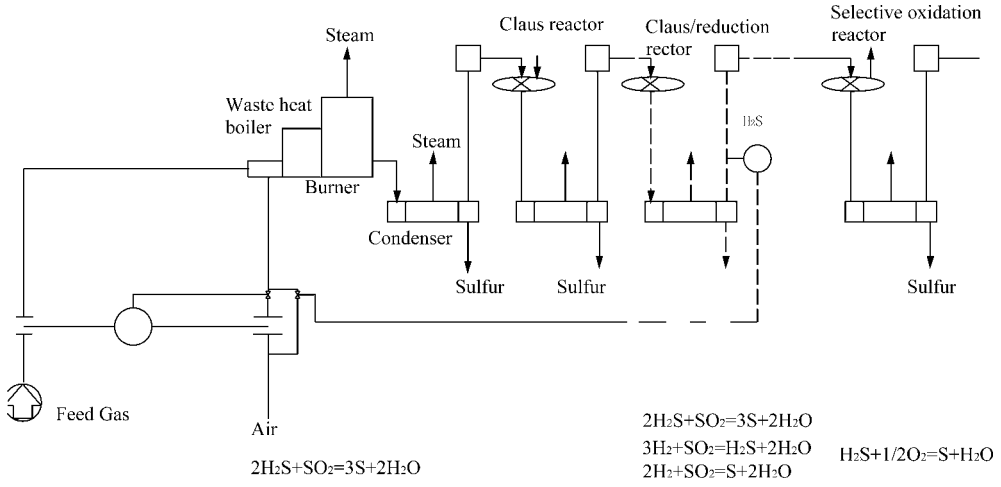

Figure 8. Flow diagram of Euro-Claus process.

stage, and the two catalytic Claus reactor stages are now with excess H_2S. The equilibrium shifts in such a way that the SO_2 concentration in the gas decreases, that is, the greater the H_2S concentration, the lower the SO_2 concentration. The SO_2 concentration in the outgas of the second Claus reactor stage is usually <0.05% (volume). H_2S in the super-Claus reactor is subsequently oxidized by air to elemental sulfur. Recovery of 98.8−99.3% H_2S in the form of elemental sulfur can be achieved during the super-Claus 99 process.[114]

4.3. Euro-Claus Process. The SO_2 present in the tail gas from the Claus reactors is unchanged because the selective oxidation catalyst oxidizes only H_2S. Taking into account the sulfur recovery and stricter environmental protection, the SO_2 concentration in the Claus reactor tail gas (feed gas to the super-Claus reactor) must be kept as low as possible. This is achieved in the super-Claus process by increasing the H_2S concentration in the Claus reactor tail gas to ∼0.8−1.5 vol %. More than that will not increase sulfur recovery further because it results in too high a bottom temperature in the super-Claus reactor, greater SO_2 formation, and lower sulfur yield.[115]

The Euro-Claus technology is an extension of the super-Claus process, which can reduce the SO_2 concentration in the Claus reactor tail gas by reducing the SO_2 to elemental sulfur. Figure 8 shows the flow diagram of the Euro-Claus process. The front end of the Euro-Claus process is composed of the well-known Claus process, while the back end consists of the well-known selective oxidation stage as applied in the super-Claus process; however, the second catalytic reactor contains a top layer of conventional Claus catalyst, positioned above a layer of hydrogenation catalyst, which facilitates conversion of SO_2 into S and H_2S.[115]

Thus, the Euro-Claus process produces elemental sulfur by three separate mechanisms: the standard Claus reaction (the bulk of the sulfur is recovered), catalytic reduction of SO_2, and selective oxidation of H_2S. Use of the hydrogenation/reduction step means that most SO_2 is eliminated; thus, H_2S is oxidized to elemental sulfur at a higher yield.[115]

5. CONCLUDING REMARKS AND PERSPECTIVES

Catalysts play a crucial role in H_2S selective catalytic oxidation. Carbon material has enriched porosity, a high specific surface area, and acidic/basic surface properties that can be modified easily, and it acts as a catalyst or catalyst support. However, it has a relatively lower temperature as an absorbent and catalyst, usually 30−80 °C, in the presence of water during discontinuous H_2S selective catalytic oxidation. Therefore, the catalyst must be regenerated periodically. Fortunately, several carbon-based catalysts have been developed for continuous H_2S selective catalytic oxidation at relatively higher temperatures. The catalytic performances of nanofibrous carbon with a herringbone structure and nitrogen-doped carbon nanotubes have been investigated. The unique advantage of a carbon-based catalyst compared with that of metal oxide-based catalysts is that the process can operate at various O_2/H_2S ratios rather than a strict stoichiometric ratio. However, the H_2S concentration and GHSV are usually very low. Moreover, factors influencing the process need to be explored further, and formation of COS and CS_2 is undesirable. Oxide-supported and metal oxide-modified titanium-, vanadium-, and iron-based oxide catalysts have been developed and investigated intensively. They have excellent catalytic activities at a relatively higher temperature range (200−300 °C) under particular H_2S/O_2 ratios. In addition, deactivation of titanium-based catalysts in the presence of water vapor and the requirement for a relatively large excess of oxygen for the iron-based super-Claus catalysts are considered the drawbacks of these oxide-based catalysts. Fortunately, a MgAlVO catalyst derived from LDH materials and intercalated clay-supported catalysts exhibit excellent catalytic activities at relatively lower temperatures. However, the influences of water, partial pressure, and porosity remain unclear. Therefore, it seems that modifying carbon material to obtain a carbon-based catalyst that can perform at high temperature under high H_2S concentrations and GHSV seems to be a promising approach. Intercalated clay and LDH-based catalysts are also considered desirable candidates.

To develop a desirable catalyst for H_2S selective catalytic oxidation, research on catalytic mechanisms and catalyst deactivation must continue. Systematic research on the catalytic mechanism using theoretical calculations and other methods is absolutely necessary. Because the catalyst plays a crucial role during H_2S catalytic oxidation, the treatment process must be developed with respect to the particular catalyst.

AUTHOR INFORMATION

Corresponding Author

*Phone: +86-10-62923564. Fax: +86-10-62923564. E-mail: zpinghao@rcees.ac.cn.

Notes

The authors declare no competing financial interest.

DOI: 10.1021/cs501476p
ACS Catal. 2015, 5, 1053−1067

■ ACKNOWLEDGMENTS

This work was financially supported by the National High Technology Research and Development Program of China (No. 2012AA063101), National Natural Science Foundation (21337003), and Science Promotion Program of Research Center for Eco-environmental Sciences, CAS (YSW2013B05).

■ REFERENCES

(1) Wiheeb, A. D.; Shamsudin, I. K.; Ahmad, M. A.; Murat, M. N.; Kim, J.; Othman, M. R. *Rev. Chem. Eng.* **2013**, *29*, 449−470.
(2) Ni, J. Q.; Heber, A. J.; Diehl, C. A.; Lim, T. T. *J. Agric Eng Res.* **2000**, *77*, 53−66.
(3) Hendrickson, R. G.; Chang, A.; Hamilton, R. J. *Am. J. Ind. Med.* **2004**, *45*, 346−350.
(4) . *Hydrogen Sulfide: Human Health Aspects; Concise International Chemical Assessment Document 53*; World Health Organization: Geneva, 2003.
(5) Garcia-Arriaga, V.; Alvarez-Ramirez, J.; Amaya, M.; Sosa, E. *Corros. Sci.* **2010**, *52*, 2268−2279.
(6) Piéplu, A.; Saur, O.; Lavalley, J. C.; Legendre, O.; Nédez, C. *Catal. Rev.: Sci. Eng.* **1998**, *40*, 409−450.
(7) El-Bishtawi, R.; Haimour, N. m. *Fuel Process. Technol.* **2004**, *8624526010.1016/j.fuproc.2004.04.001*.
(8) Khudenko, B. M.; Gitman, G. M.; Wechsler, T. E. P. *J. Environ. Eng.* **1993**, *119*, 1233−1251.
(9) Laperdrix, E.; Costentin, G.; Saur, O.; Lavalley, J. C.; Nédez, C.; Savin-Poncet, S.; Nougayrède, J. *J. Catal.* **2000**, *189*, 63−69.
(10) Eow, J. S. *Environ. Prog. Sustain.* **2002**, *21*, 143−162.
(11) Steijns, M.; Mars, P. *J. Catal.* **1974**, *35*, 11−17.
(12) Kaliva, A. N.; Smith, J. W. *Can. J. Chem. Eng.* **1983**, *61*, 208−212.
(13) Meeyoo, V.; Trimm, D. L.; Cant, N. W. *J. Chem. Technol. Biotechnol.* **1997**, *68*, 411−416.
(14) Primavera, A.; Trovarelli, A.; Andreussi, P.; Dolcetti, G. *Appl. Catal., A* **1998**, *173*, 185−192.
(15) Adib, F.; Bagreev, A.; Bandosz, T. J. *J. Colloid Interface Sci.* **1999**, *216*, 360−369.
(16) Bashkova, S.; Armstrong, T. R.; Schwartz, V. *Energy Fuels* **2009**, *23*, 1674−1682.
(17) Bashkova, S.; Baker, F. S.; Wu, X.; Armstrong, T. R.; Schwartz, V. *Carbon* **2007**, *45*, 1354−1363.
(18) Wu, X. X.; Schwartz, V.; Overbury, S. H.; Armstrong, T. R. *Energy Fuels* **2005**, *19*, 1774−1782.
(19) Klein, J.; Henning, K. D. *Fuel* **1984**, *63*, 1064−1067.
(20) Adib, F.; Bagreev, A.; Bandosz, T. J. *Langmuir* **1999**, *16*, 1980−1986.
(21) Fang, H. B.; Zhao, J. T.; Fang, Y. T.; Huang, J. J.; Wang, Y. *Fuel* **2013**, *108*, 143−148.
(22) Tsai, J. H.; Jeng, F. T.; Chiang, H. L. *Adsorpt.: J. Int. Adsorpt. Soc.* **2001**, *7*, 357−366.
(23) Chiang, H. L.; Tsai, J. H.; Tsai, C. L.; Hsu, Y. C. *Sep. Sci. Technol.* **2000**, *35*, 903−918.
(24) Henning, K. D.; Schäfer, S. *Sep. Purif. Technol.* **1993**, *7*, 235−240.
(25) Cal, M. P.; Strickler, B. W.; Lizzio, A. A. *Carbon* **2000**, *38*, 1757−1765.
(26) Bandosz, T. J.; Bagreev, A. *Abstracts of Papers*; 228th National Meeting of the American Chemical Society, Philadelphia, PA, Aug 22−26, 2004, American Chemical Society: Washington, DC, 2004, FUEL 156.
(27) Seredych, M.; Bandosz, T. J. *Mater. Chem. Phys.* **2009**, *113*, 946−952.
(28) Pigamo, A.; Besson, M.; Blanc, B.; Gallezot, P.; Blackburn, A.; Kozynchenko, O.; Tennison, S.; Crezee, E.; Kapteijn, F. *Carbon* **2002**, *40*, 1267−1278.
(29) Szymański, G. S.; Karpiński, Z.; Biniak, S.; Świątkowski, A. *Carbon* **2002**, *40*, 2627−2639.
(30) Strelko, V., Jr; Malik, D. J.; Streat, M. *Carbon* **2002**, *40*, 95−104.
(31) Nhut, J. M.; Nguyen, P.; Pham-Huu, C.; Keller, N.; Ledoux, M. J. *Catal. Today* **2004**, *91*−*2*, 91−97.
(32) Bagreev, A.; Bandosz, T. J. *Ind. Eng. Chem. Res.* **2002**, *41*, 672−679.
(33) Mikhalovsky, S. V.; Zaitsev, Y. P. *Carbon* **1997**, *35*, 1367−1374.
(34) Biniak, S.; Szymanski, G.; Siedlewski, J.; Swiatkowski, A. *Carbon* **1997**, *35*, 1799−1810.
(35) Xiao, Y.; Wang, S.; Wu, D.; Yuan, Q. *Sep. Purif. Technol.* **2008**, *59*, 326−332.
(36) Xiao, Y.; Wang, S.; Wu, D.; Yuan, Q. *J. Hazard. Mater.* **2008**, *153*, 1193−1200.
(37) Gardner, T. H.; Berry, D. A.; David Lyons, K.; Beer, S. K.; Freed, A. D. *Fuel* **2002**, *81*, 2157−2166.
(38) Wu, X.; Kercher, A. K.; Schwartz, V.; Overbury, S. H.; Armstrong, T. R. *Carbon* **2005**, *43*, 1087−1090.
(39) George, Z. M. *J. Catal.* **1974**, *35*, 218−224.
(40) Chiang, H. L.; Tsai, J. H.; Tsai, C. L.; Hsu, Y. C. *Sep. Purif. Technol.* **2000**, *35*, 903−918.
(41) Bandosz, T. J.; Bagreev, A.; Adib, F.; Turk, A. *Environ. Sci. Technol.* **2000**, *34*, 1069−1074.
(42) Bagreev, A.; Bandosz, T. J. *Ind. Eng. Chem. Res.* **2005**, *44*, 530−538.
(43) Rhodes, C.; Riddel, S. A.; West, J.; Williams, B. P.; Hutchings, G. J. *Catal. Today* **2000**, *59*, 443−464.
(44) Sun, F.; Liu, J.; Chen, H.; Zhang, Z.; Qiao, W.; Long, D.; Ling, L. *ACS Catal.* **2013**, *3*, 862−870.
(45) Iijima, S. *Nature* **1991**, *354*, 56.
(46) Ledoux, M. J.; Vieira, R.; Pham-Huu, C.; Keller, N. *J. Catal.* **2003**, *216*, 333−342.
(47) Nhut, J. M.; Pesant, L.; Tessonnier, J. P.; Winé, G.; Guille, J.; Pham Huu, C.; Ledoux, M. J. *Appl. Catal., A* **2003**, *254*, 345−363.
(48) Chen, Q.; Wang, J.; Liu, X.; Zhao, X.; Qiao, W.; Long, D.; Ling, L. *Carbon* **2011**, *49*, 3773−3780.
(49) Chizari, K.; Deneuve, A.; Ersen, O.; Florea, I.; Liu, Y.; Edouard, D.; Janowska, I.; Begin, D.; Cuong, P. H. *ChemSusChem* **2012**, *5*, 102−108.
(50) De Jong, K. P.; Geus, J. W. *Catal. Rev.-Sci. Eng.* **2000**, *42*, 481−510.
(51) Dalai, A. K.; Majumdar, A.; Chowdhury, A.; Tollefson, E. L. *Can. J. Chem. Eng.* **1993**, *71*, 75−82.
(52) Kuvshinov, G. G.; Moguilnykh, J. I.; Lebedev, M. J.; Kuvshinov, D. G.; Zavarukhin, S. G. Russian Patent Application 2111164, 1997.
(53) Kuvshinov, G. G.; Shinkarev, V. V.; Glushenkov, A. M.; Boyko, M. N.; Kuvshinov, D. G. *Particuology* **2006**, *4*, 70−72.
(54) Shinkarev, V. V.; Glushenkov, A. M.; Kuvshinov, D. G.; Kuvshinov, G. G. *Appl. Catal., B* **2009**, *85*, 180−191.
(55) Shinkarev, V. V.; Glushenkov, A. M.; Kuvshinov, D. G.; Kuvshinov, G. G. *Carbon* **2010**, *48*, 2004−2012.
(56) Chen, Q.; Wang, Z.; Long, D.; Liu, X.; Zhan, L.; Liang, X.; Qiao, W.; Ling, L. *Ind. Eng. Chem. Res.* **2010**, *49*, 3152−3159.
(57) Davydov, A. A.; Marshneva, V. I.; Shepotko, M. L. *Appl. Catal., A* **2003**, *244*, 93−100.
(58) Uhm, J. H.; Shin, M. Y.; Zhidong, J.; Chung, J. S. *Appl. Catal., B* **1999**, *22*, 293−303.
(59) Laperdrix, E.; Costentin, G.; Nguyen, N.; Studer, F.; Lavalley, J. C. *Catal. Today* **2000**, *61*, 149−155.
(60) Koyuncu, D. D. E.; Yasyerli, S. *Ind. Eng. Chem. Res.* **2009**, *48*, 5223−5229.
(61) Li, K. T.; Yen, C. S.; Shyu, N. S. *Appl. Catal., A* **1997**, *156*, 117−130.
(62) Jung, S. J.; Kim, M. H.; Chung, J. K.; Moon, M. J.; Chung, J. S.; Park, D. W.; Woo, H. C. In *Nanotechnology in Mesostructured Materials*; Park, S. E., Ryoo, R., Ahn, W. S., Lee, C. W., Chang, J. S., Eds.; Studies in Surface Science and Catalysis; Elsevier: Amsterdam, 2003; Vol. *146*; p 621.
(63) Kersen, U.; Keiski, R. L. *Catal. Commun.* **2009**, *10*, 1039−1042.
(64) Reyes-Carmona, Á.; Soriano, M. D.; López Nieto, J. M.; Jones, D. J.; Jiménez-Jiménez, J.; Jiménez-López, A.; Rodríguez-Castellón, E. *Catal. Today* **2013**, *210*, 117−123.
(65) Li, K. T.; Huang, M. Y.; Cheng, W. D. *Ind. Eng. Chem. Res.* **1996**, *35*, 621−626.

DOI: 10.1021/cs501476p
ACS Catal. 2015, 5, 1053−1067

(66) Shin, M. Y.; Park, D. W.; Chung, J. S. *Appl. Catal., B* **2001**, *30*, 409−419.
(67) Soriano, M. D.; Rodríguez-Castellón, E.; García-González, E.; López Nieto, J. M. *Catal. Today* **2014**, *238*, 62−68.
(68) Soriano, M. D.; López Nieto, J. M.; Ivars, F.; Concepción, P.; Rodríguez-Castellón, E. *Catal. Today* **2012**, *192* (1), 28−35.
(69) Li, K. T.; Chi, Z. H. *Appl. Catal., A* **2001**, *206*, 197−203.
(70) Morss, L. R. In *Handbook of the Physics and Chemistry of Rare Earths*; Gschneidner, K. A., Eyring, L., Choppin, G. R., Lander, G. H., Eds.; Elsevier: Amsterdam, 1994; Vol. *18*, p 239.
(71) *Standard Potentials in Aqueous Solution*; Bard, A. J., Parson, R., Jordan, J., Eds.; Marcel Dekker: New York, 1986.
(72) Shriver, D. F., Arkins, P., Langford, C. H. *Inorganic Chemistry*; W. H. Freeman and Company: New York, 1994; p 37.
(73) Yasyerli, S.; Dogu, G.; Dogu, T. *Catal. Today* **2006**, *117*, 271−278.
(74) Li, K. T.; Huang, C. H. *Ind. Eng. Chem. Res.* **2006**, *45*, 7096−7100.
(75) Li, K. T.; Wu, R. S. *Ind. Eng. Chem. Res.* **2001**, *40*, 1052−1057.
(76) Zhang, X.; Wang, Z.; Qiao, N. L.; Qu, S. Q.; Hao, Z. P. *ACS Catal.* **2014**, *4*, 1500−1510.
(77) Xu, Z. P.; Zhang, J.; Adebajo, M. O.; Zhang, H.; Zhou, C. H. *Appl. Clay Sci.* **2011**, *53*, 139−150.
(78) Zhou, C. H. *Appl. Clay Sci.* **2011**, *53*, 87−96.
(79) Wang, S. H.; Wang, Y. B.; Dai, Y. M.; Jehng, J. M. *Appl. Catal., A* **2012**, *439*−*440*, 135−141.
(80) Terörde, R. J. A. M.; van den Brink, P. J.; Visser, L. M.; van Dillen, A. J.; Geus, J. W. *Catal. Today* **1993**, *17*, 217−224.
(81) Chun, S. W.; Jang, J. Y.; Park, D. W.; Woo, H. C.; Chung, J. S. *Appl. Catal., B* **1998**, *16*, 235−243.
(82) Shin, M. Y.; Park, D. W.; Chung, J. S. *Catal. Today* **2000**, *63*, 405−411.
(83) Shin, M. Y.; Nam, C. M.; Park, D. W.; Chung, J. S. *Appl. Catal., A* **2001**, *211*, 213−225.
(84) Terörde, R. J. A. M.; de Jong, M. C.; Crombag, M. J. D.; van den Brink, P. J.; van Dillen, A. J.; Geus, J. W. In *New Developments in Selective Oxidation II*; Corberán, V. C., Bellón, S. V., Eds.; Studies in Surface Science and Catalysis; Elsevier: Amsterdam, 1993; Vol. *82*; p 861.
(85) Bukhtiyarova, G. A.; Delii, I. V.; Sakaeva, N. S.; Kaichev, V. V.; Plyasova, L. M.; Bukhtiyarov, V. I. *React. Kinet. Mech. Catal.* **2007**, *92*, 89−97.
(86) Berben, P. H. Ph.D. Thesis, University of Utrecht, 1992.
(87) Batygina, M. V.; Dobrynkin, N. M.; Kirichenko, O. A.; Khairulin, S. R.; Ismagilov, Z. R. *React. Kinet. Mech. Catal.* **1992**, *48*, 55−63.
(88) Song, M. W.; Kang, M.; Kim, K. L. *React. Kinet. Mech. Catal.* **2003**, *78*, 365−371.
(89) Grabowski, R.; Grzybowska, B.; Samson, K.; Sloczynski, J.; Stoch, J.; Wcislo, K. *Appl. Catal., A* **1995**, *125*, 129−144.
(90) Bineesh, K. V.; Kim, D. K.; Kim, D. W.; Cho, H. J.; Park, D. W. *Energy Environ. Sci.* **2010**, *3*, 302−310.
(91) Bineesh, K. V.; Kim, S. Y.; Jermy, B. R.; Park, D. W. *J. Mol. Catal. A: Chem.* **2009**, *308*, 150−158.
(92) Bineesh, K. V.; Kim, D. K.; Kim, M.I. L.; Park, D. W. *Appl. Clay Sci.* **2011**, *53*, 204−211.
(93) Bineesh, K. V.; Kim, S. Y.; Jermy, B. R.; Park, D. W. *J. Ind. Eng. Chem.* **2009**, *15*, 207−211.
(94) Bineesh, K. V.; Kim, D. K.; Kim, M. I.; Selvaraj, M.; Park, D. W. *Dalton Trans.* **2011**, *40*, 3938−3945.
(95) Bineesh, K. V.; Kim, M. I. L.; Park, M. S.; Lee, K. Y.; Park, D. W. *Catal. Today* **2011**, *175*, 183−188.
(96) Zhang, X.; Dou, G. Y.; Wang, Z.; Li, L.; Wang, Y. F.; Wang, H. L.; Hao, Z. P. *J. Hazard. Mater.* **2013**, *260*, 104−111.
(97) Zhang, X.; Dou, G. Y.; Wang, Z.; Cheng, J.; Wang, H. L.; Ma, C. Y.; Hao, Z. P. *Catal. Sci. Technol.* **2013**, *3*, 2778−2785.
(98) Soriano, M. D.; Jimenez-Jimenez, J.; Concepcion, P.; Jimenez-Lopez, A.; Rodriguez-Castellon, E.; Nieto, J. M. L. *Appl. Catal., B* **2009**, *92*, 271−279.
(99) Holgado, J. P.; Soriano, M. D.; Jiménez-Jiménez, J.; Concepción, P.; Jiménez-López, A.; Caballero, A.; Rodríguez-Castellón, E.; Nieto, J. M. L. *Catal. Today* **2010**, *155*, 296−301.
(100) León, M.; Jiménez-Jiménez, J.; Jiménez-López, A.; Rodríguez-Castellón, E.; Soriano, D.; López Nieto, J. M. *Solid State Sci.* **2010**, *12*, 996−1001.
(101) Palma, V.; Barba, D.; Ciambelli, P. In *Chemical Engineering Transactions*; Proceedings of 11th International Conference on Chemical and Process Engineering, Milan, Italy, Jun 02−05, 2013; Pierucci, S., Klemes, J. J., Eds.; Aidic Servizi Srl: Milano, 2013.
(102) Palma, V.; Barba, D. *Fuel* **2014**, *135*, 99−104.
(103) Nguyen, P.; Edouard, D.; Nhut, J. M.; Ledoux, M. J.; Pham, C.; Pham-Huu, C. *Appl. Catal., B* **2007**, *76*, 300−310.
(104) Ghosh, T. K.; Tollefson, E. L. *Can. J. Chem. Eng.* **1986**, *64*, 969−976.
(105) Steijns, M.; Derks, F.; Verloop, A.; Mars, P. *J. Catal.* **1976**, *42*, 87−95.
(106) Zhenglu, P.; Weng, H.-S.; Han-Yu, F.; Smith, J. M. *AlChE J.* **1984**, *30*, 1021−1025.
(107) Yan, R.; Liang, D. T.; Tsen, L.; Tay, J. H. *Environ. Sci. Technol.* **2002**, *36*, 4460−4466.
(108) Yan, R.; Chin, T.; Ng, Y. L.; Duan, H.; Liang, D. T.; Tay, J. H. *Environ. Sci. Technol.* **2003**, *38*, 316−323.
(109) Dudzik, Z.; Ziólek, M. *J. Catal.* **1978**, *51*, 345−354.
(110) Dudzik, Z.; Bilska-Ziolek, M.; Czeremuzinska, J. *Bull. Acad. Polym. Sci.* **1974**, *22*, 307.
(111) Satterfield, C. N. *Heterogeneous Catalysis in Industrial Practice*; Krieger Publishing Company: Malabar, FL, 1996; p 269.
(112) Borsboom, J.; Lagas, J. A. Presented at 22nd ACHEMA Exhibition Congress, Frankfurt, 1988.
(113) Borsboom, J.; Goar, B. G.; Heijkoop, G.; Lagas, J. A. *Sulphur* **1992**, *220*, 44−47.
(114) Pandey, R. A.; Malhotra, S. *Crit. Rev. Environ. Sci. Technol.* **1999**, *29*, 229−268.
(115) Anonymous. *Sulphur* **2000**, *270*, 65−72.

DOI: 10.1021/cs501476p
ACS Catal. 2015, 5, 1053−1067